Neutron single-particle strength in silicon isotopes: Constraining the driving forces of shell evolution

S. R. Stroberg, A. Gade, J. A. Tostevin, V. M. Bader, T. Baugher, D. Bazin, J. S. Berryman, B. A. Brown, C. M. Campbell, K. W. Kemper, C. Langer, E. Lunderberg, A. Lemasson, S. Noji, T. Otsuka, F. Recchia, C. Walz, D. Weisshaar, and S. Williams

Neutron single-particle strength in silicon isotopes: constraining the driving forces of shell evolution

S.R. Stroberg,[1, 2, *] A. Gade,[1, 2] J.A. Tostevin,[3] V.M. Bader,[1, 2] T. Baugher,[1, 2] D. Bazin,[1, 2]
J.S. Berryman,[1] B.A. Brown,[1, 2] C.M. Campbell,[4] K.W. Kemper,[5] C. Langer,[1, 6] E. Lunderberg,[1, 2]
A. Lemasson,[1] S. Noji,[1] T. Otsuka,[7, 8, 1] F. Recchia,[1] C. Walz,[1] D. Weisshaar,[1] and S. Williams[1]

[1] *National Superconducting Cyclotron Laboratory, Michigan State University, East Lansing, Michigan 48824, USA*
[2] *Department of Physics and Astronomy, Michigan State University, East Lansing, Michigan 48824, USA*
[3] *Faculty of Engineering and Physical Sciences, University of Surrey, Guildford, Surrey, GU2 7XH, United Kingdom*
[4] *Lawrence Berkeley National Laboratory, Berkeley, California 94720, USA*
[5] *Department of Physics, Florida State University, Tallahassee, Florida 32306, USA*
[6] *Joint Institute for Nuclear Astrophysics, Michigan State University, East Lansing, Michigan 48824, USA*
[7] *Department of Physics, University of Tokyo, Hongo, Bunkyo-ku, Tokyo 113-0033, Japan*
[8] *Center for Nuclear Physics, University of Tokyo, Hongo, Bunkyo-ku, Tokyo 113-0033, Japan*

Shell evolution is studied in the neutron-rich silicon isotopes ^{36,38,40}Si using neutron single-particle strengths deduced from one-neutron knockout reactions. Configurations involving neutron excitations across the $N = 20$ and $N = 28$ shell gaps are quantified experimentally in these rare isotopes. Comparisons with shell model calculations show that the tensor force, understood to drive the collective behavior in ^{42}Si with $N = 28$, is already important in determining the structure of ^{40}Si with $N = 26$. New data relating to cross-shell excitations provide the first quantitative support for repulsive contributions to the cross-shell $T = 1$ interaction arising from three-nucleon forces.

The atomic nucleus is a fermionic many-body quantum system composed of strongly-interacting protons and neutrons. Large stabilizing energy gaps, separating clusters of single-particle states, provide the cornerstone for the nuclear shell model, one of the most powerful tools available for describing the structure of atomic nuclei. In the simplest version of the shell model, empirical shell gaps at the *magic* nucleon numbers 2, 8, 20, 28, 50, 82, and 126 are reproduced when assuming that the nucleons experience, predominantly, a mean-field potential with an attractive one-body spin-orbit term.

In rare isotopes, with imbalanced proton and neutron numbers, significant modifications have been observed. Here, new shell gaps develop and the conventional gaps at the magic numbers can collapse. Understanding this observed evolution is key to a comprehensive description of atomic nuclei across the nuclear chart. Detailed studies of the evolution of shell structure with proton number (Z) or neutron number (N), e.g. [1], probe the effects of particular components of the complex interactions between nucleons: such as the spin-isospin [2] and tensor [3] two-body terms, and three-body force terms [4, 5]. The need to include such terms in the nuclear interaction has been demonstrated by their robust effects that become amplified at large isospin [3, 5] and, without which, features such as driplines and shell structure may not be reproduced. Clearly, a full treatment of the nuclear force from its underlying QCD degrees of freedom is very challenging, and experimental data is essential in helping to identify the most important degrees of freedom responsible for driving the evolution of nuclear properties.

Here, we present data for the silicon ($Z = 14$) isotopic chain, a region of the nuclear chart were rapid shell evolution is at play. ^{34}Si is known to exhibit closed-shell behavior while ^{42}Si shows no indication of an $N = 28$ shell gap [6]. Hitherto, observations on the neutron-rich silicon isotopes, dominated by measurements of collective observables, have been reproduced by large-scale shell model calculations using phenomenological effective interactions [6–9]. To assess the theoretical description of the evolving shell structure it is also critical to investigate these nuclei using single-particle observables, such as the energies and single-particle (spectroscopic) strengths of states involving the active orbitals at shell gaps.

This Rapid Communication reports a first experimental investigation of observables that reflect single-neutron degrees of freedom in the ^{36,38,40}Si isotopes. Extraction of the presented cross-sections from the data, collected in the measurement reported in Ref. [10], required the development of novel analysis strategies. The results go beyond those of Ref. [10], and are interpreted here within a common theoretical framework. Exclusive one-neutron knockout cross sections, measured using γ-ray tagged neutron removal reactions from ^{36,38,40}Si projectiles, are used to identify and quantify configurations that involve neutron excitations across the $N = 20$ and $N = 28$ shell gaps. Specifically, the partial cross sections to the lowest-lying $7/2^-$ and $3/2^-$ states, involving the diminishing $N = 28$ gap, and $1/2^+$ and $3/2^+$ states, involving the $N = 20$ shell gap, are measured and compared to calculations using shell-model spectroscopic strengths and eikonal reaction theory. The results (i) track the evolution of the neutron $f_{7/2}$ and $p_{3/2}$ orbitals at the $N = 28$ shell gap, and (ii) quantify the little-explored neutron excitations, from the $d_{3/2}$ and $s_{1/2}$ sd-shell orbitals, across the $N = 20$ gap.

___

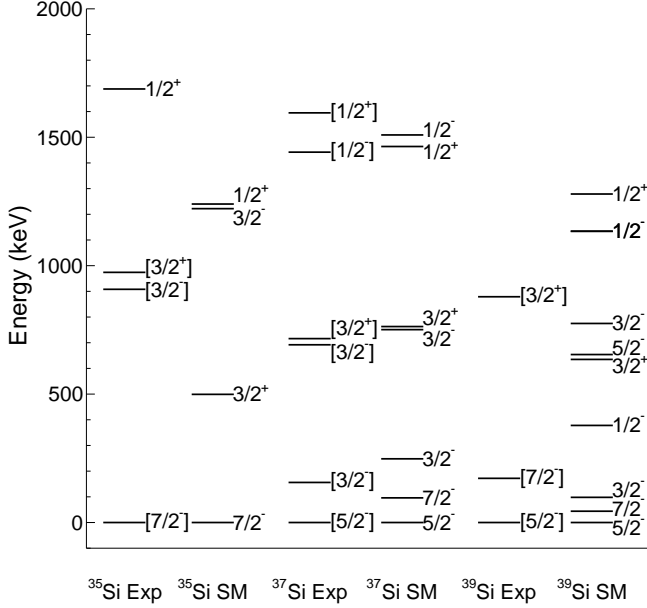* Present address: TRIUMF, Vancouver, British Columbia V6T 2A3, Canada

FIG. 1. Experimental level schemes for low-lying states in ^{35}Si, ^{37}Si and ^{39}Si, compared with shell model calculations using the SDPF-MU effective interaction [10].

The experiment was performed at the Coupled Cyclotron Facility of the National Superconducting Cyclotron Laboratory at Michigan State University. Secondary beams of ^{36,38,40}Si, produced by fast fragmentation of a ^{48}Ca primary beam, impinged on a beryllium target with energies of 100, 95 and 85 MeV/u, respectively. The one-neutron knockout residues were detected and identified on an event-by-event basis. Prompt γ-rays, emitted in-flight from de-excitation of the knockout residues, were detected with the GRETINA array [11] surrounding the target position, and were Doppler-corrected event-by-event.

The level schemes of the knockout residues were constructed based on $\gamma\gamma$ coincidences, energy sums, and intensity balances. These are summarized in Fig. 1. Spin-parity assignments were made with the aid of the parallel momentum distributions of the residues in comparison with theoretical distributions calculated in an eikonal model according to the formalism of Ref. [12]. Full details of the experiment, data analysis and the spin-parity assignments can be found in Ref. [10].

The knockout cross sections to negative parity states, i.e. removal from the neutron $f_{7/2}$ and $p_{3/2}$ orbitals in ^{36,38,40}Si, map their spectroscopic strengths. The experimental and calculated cross sections are listed in Table I. Details of the shell model calculations used can be found in Ref. [10]. Determining the partial cross sections is challenging in some cases. For example, population of the ^{35}Si($7/2_1^-$) ground state is hindered by the presence of a $3/2^+$ isomer, expected to be strongly populated but which cannot be tagged with prompt in-beam γ spectroscopy. We use instead the ^{35}Si residue momentum
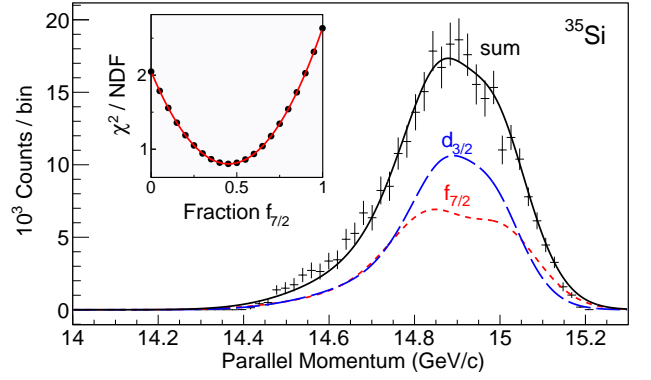

FIG. 2. (color online) Momentum distribution of the ^{35}Si residues produced in the ground state and any isomers following one neutron knockout from ^{36}Si. The curves show a fit using a linear combination of the calculated distributions for removal from the $f_{7/2}$ and $d_{3/2}$ orbits.

TABLE I. Experimental (σ_{exp}) and calculated (σ_{th}) one-neutron knockout cross sections to the lowest $7/2^-$ and $3/2^-$ states in the mass A_{res} residues. The σ_{th} use the shell-model spectroscopic factors C^2S and their center-of-mass correction, $(A_{proj}/A_{res})^3$, and the calculated eikonal model single-particle cross sections σ_{sp}. All cross sections are in millibarns.

| J_f^π | A_{proj} | A_{res} | σ_{sp} | SDPF-MU | | SDPF-U | | σ_{exp} |
				C^2S	σ_{th}	C^2S	σ_{th}	
$7/2_1^-$	36	35	15.7	1.71	29.2	1.73	29.5	23(6)
	38	37	15.2	2.81	46.3	2.85	46.6	47(9)
	40	39	15.0	3.19	51.8	3.33	53.9	49(7)
	42	41	15.9[a]	2.73	46.6	3.70	64.1	
$3/2_1^-$	36	35	17.8	0.13	2.6	0.09	1.8	8(3)
	38	37	20.1	0.11	2.4	0.02	0.4	9(7)
	40	39	21.7[a]	0.90	21.3	0.51	12.2	29(20)
	42	41	26.7[a]	1.72	49.4	0.03	1.0	
$3/2_2^-$	38	37	18.8	0.27	5.5	0.27	5.6	7(3)
	40	39	19.8[a]	0.08	1.8	0.17	3.7	
	42	41	22.6[a]	0.19	4.6	1.02	30.5	

[a] Experimental excitation energy not known. σ_{sp} is calculated with the SDPF-MU shell model energy.

distribution to extract the population fraction. Fig. 2 shows the ^{35}Si parallel momentum distribution after the subtraction of all events that decay by prompt γ emission. Overlaid is a linear combination of the theoretical distributions for neutron removal from the $f_{7/2}$ and $d_{3/2}$ orbits together with the resulting χ^2 fit minimization, giving a $f_{7/2}$ fraction of 0.45(10). The ground state cross section is estimated from this fraction of the knockout reaction events with no prompt γ decay.

The ^{37}Si($3/2_1^-$) and ^{39}Si($7/2_1^-$) states are nanosecond isomers. As a result, their depopulating transitions have broad, asymmetric peak shapes due to the larger uncertainty in the position and velocity of the decaying fragment and corresponding degradation of the Doppler reconstruction. This lifetime effect is incorporated into the

GEANT4 [13] simulation and a best-fit lifetime is obtained with a maximum likelihood method. An example is shown in Fig. 3. The proximity of these peaks to the γ-ray detection threshold results in a dependence of the extracted peak intensity on the assumed lifetime. This dependence is shown in the lower panel of Fig. 3(a), and makes the major contribution to the uncertainty in these peak intensities. The effect of the lifetime on the peak shape depends on the polar angle of the emitted γ ray. We can confirm that the simulation reproduces this dependence by dividing the array into three rings centered near 50, 65 and 90 degrees (labeled front, middle, and backward in Fig. 3), and comparing the fit in each ring. This comparison, in Fig. 3(b), shows satisfactory agreement.
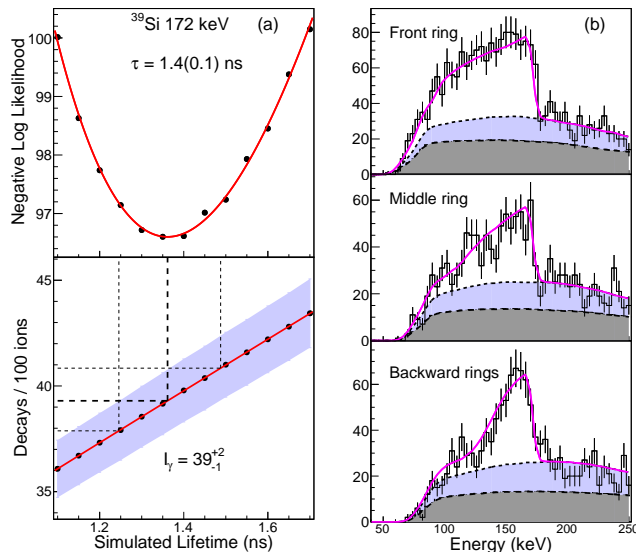

FIG. 3. (color online) (a) Maximum likelihood fit to the lifetime of the state in ^{39}Si decaying by a 172 keV γ ray. Only statistical uncertainties are shown. The lower panel shows the influence of the uncertainty in lifetime upon the uncertainty in the number of decays, where the error band shows the uncertainty in the fit. (b) The resulting spectra in the front, middle and backward rings of GRETINA using the best-fit lifetime. The shaded gray area indicates the continuous background from target breakup, the blue area indicates the Compton continuum of all higher-lying peaks, and the magenta curve indicates the total fit [10].

The large uncertainty for the ^{39}Si$(3/2^-_1)$ state in Table I is due to several observed transitions which were not placed in the level scheme, introducing ambiguity in the subtraction procedure described above. The quoted uncertainty includes the range of possible level schemes which are consistent with the data. Further, since the second $3/2^-$ state was not identified, the value shown provides only a lower limit on the bound $p_{3/2}$ strength. The stated ^{37,39}Si$(7/2^-)$ cross sections assume that population of the predicted $5/2^-_1$ states is small compared to other sources of uncertainty (the shell model strengths predict cross sections of order 1 mb). The measured
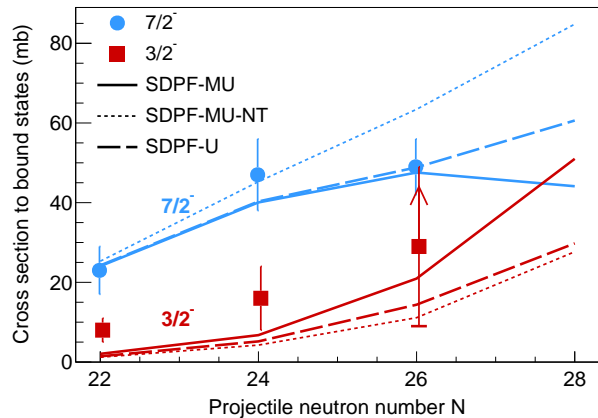

FIG. 4. (color online) One-neutron knockout reaction partial cross sections to bound final states with $J^\pi = 7/2^-$ and $3/2^-$, as a function of the neutron number of the silicon projectile. The arrow, for $N = 26$, indicates a lower limit. Theoretical predictions using the SDPF-MU (solid lines) and SDPF-U (dashed lines) effective interactions are also shown. The dotted line (SDPF-MU-NT) results when the tensor component of the cross-shell sd-fp interaction of SDPF-MU is set to zero. All theoretical curves have been scaled by the observed knockout reaction systematics (see text).

and theoretical cross sections (for the SDPF-MU [8] and SDPF-U [7] shell model effective interactions) are shown in Fig. 4. In the region of ^{42}Si, the tensor component of the interaction has been proposed as an important driving force for shell evolution [3, 6], and so we investigate this with a third set of calculations—denoted SDPF-MU-NT—obtained by removing the tensor part of the cross-shell sd-fp interaction of SDPF-MU. All theoretical cross sections are scaled by an empirical quenching factor $R(\Delta S)$ obtained from a fit to the knockout reaction systematics [10, 14].

The agreement between the measured $7/2^-$ state cross sections (shown in blue) and both the SDPF-MU and SDPF-U calculations is excellent. We see that the effect of the tensor force, as discussed in [3], becomes important [15] already around ^{40}Si. In contrast, the $3/2^-$ state cross sections (shown in red) are markedly underpredicted. This finding is consistent with previous measurements using one-neutron knockout, from ^{30,32}Mg [16] and ^{33}Mg [17], as well as a (t, p) transfer measurement populating states in ^{32}Mg [18]. In each of these cases, an excess of $p_{3/2}$ strength was seen, relative to shell model predictions, while the $f_{7/2}$ strength was generally consistent with the shell model. The fact that this discrepancy is observed for different reaction mechanisms, and only for a particular orbit, suggests that this is a structure effect and not related to any systematic defect of the reaction theory. As can be seen from the dotted line in Fig. 4, the tensor force does not appear to have much effect in ^{36}Si and ^{38}Si, and so the $p_{3/2}$ discrepancy likely has origins elsewhere.

TABLE II. Experimental (σ_{exp}) and calculated (σ_{th}) one-neutron knockout cross sections to the lowest $3/2^+$ and $1/2^+$ states in the mass A_{res} residues. The σ_{th} use the shell-model spectroscopic factors C^2S and their center-of-mass correction, $(A_{proj}/A_{res})^2$, and the calculated eikonal model single-particle cross sections σ_{sp}. All cross sections are in millibarns.

				SDPF-MU		SDPF-U		
J_f^π	A_{proj}	A_{res}	σ_{sp}	C^2S	σ_{th}	C^2S	σ_{th}	σ_{exp}
$3/2_1^+$	36	35	14.2	3.07	46.0	2.61	39.2	29(6)
	38	37	13.8	2.79	40.6	2.19	28.4	19(2)
	40	39	13.3	2.31	32.4	1.69	19.9	14(2)
$1/2_1^+$	36	35	21.1	0.96	21.3	1.00	22.3	13(1)
	38	37	20.7	0.80	17.5	0.97	19.5	10(1)
	40	39	22.7[a]	0.53	12.6	0.72	14.1	

[a] Experimental excitation energy not known. σ_{sp} is calculated with the SDPF-MU shell model energy.

To clarify the $N = 20$ shell closure we also consider the removal of neutrons from the $d_{3/2}$ and $s_{1/2}$ sd-shell orbitals, populating positive-parity final states. The cross sections for population of bound $3/2^+$ and $1/2^+$ states are listed in Table II. The large uncertainty for the ^{35}Si($3/2_1^+$) state yield is due to the same isomer effect as was discussed for the $7/2_1^-$ state. The measured and theoretical (SDPF-MU and SDPF-U) cross sections are compared in Table II. Both model calculations, which include $1p-1h$ excitations from the sd-shell in the wave functions of the residual nuclei, over-predict the strength of transitions from these orbits.

It is very likely that the theoretical over-prediction of sd-shell strength and the aforementioned under-prediction of fp-shell strength are related, reflecting unaccounted-for excitations across the $N = 20$ shell gap in the ground states of the projectiles. Indeed, the present calculations for the projectile ground states were performed in a $0\hbar\omega$ model space in which the neutron sd-shell orbits are fixed and fully occupied. So, it is evident that the assumed occupation of sd-shell orbits is too high. In the Monte Carlo shell model calculations of Ref. [19], that allowed an arbitrary number of neutron particle-hole excitations from the sd-shell into the lower fp shell, the results, in ^{36,38}Si, were an average excess of approximately $0.3-0.4$ neutrons compared to normal filling. This reduced sd strength (and additional fp strength) would bring the shell-model predictions into better agreement with the present data, with the exception of the large $3/2^+$ strength of SDPF-MU.

Finally, the newly-measured energies of the $3/2^+$ and $1/2^+$ hole states provide guidance for shell-model effective interactions that include excitations across the $N = 20$ shell gap. Figure 5 shows the experimental energies of the $3/2_1^+$ ($1/2_1^+$) states relative to the $7/2_1^-$ states, indicative of the $f_{7/2}$ to $d_{3/2}$ ($s_{1/2}$) shell gap. For reference, we also show the shell-model spectroscopic factors for populating these states by one-neutron removal. The experimental data indicate that both gaps shrink as neu-

trons are added from $N = 19$ to 25, while SDPF-MU predicts a flat trend and SDPF-U predicts an increase of these gaps.

These qualitatively different predictions can largely be attributed to a difference in the cross-shell neutron-neutron ($T = 1$) interaction. Figure 6 shows selected monopole (i.e. angle-averaged) terms of the SDPF-U and SDPF-MU interactions. While both interactions have similar sd and fp monopoles and are successful in reproducing the spectroscopy of the region within the $0\hbar\omega$ model space, the more-attractive SDPF-U cross-shell monopoles over-bind the neutron sd orbits as neutrons are added to the fp shell, leading to the observed trend. This discrepancy highlights a key difference between the two interactions. In SDPF-U, due to insufficient experimental data, the cross-shell part of the interaction was left as essentially the two-body G matrix. On the other hand, the cross-shell component of SDPF-MU was generated from the schematic potential V_{MU} [20] which allowed—by incorporating information from data closer to stability—the approximate inclusion of the repulsive contribution of three body forces to the effective $T = 1$ two body interaction. This same repulsive $T = 1$ effect has been shown to be robust consequence of the Fujita-Miyazawa process which is crucial in reproducing the oxygen dripline [5]. We note that a more recent version of SDPF-U [9], developed to allow neutron excitations across the $N = 20$ gap, in fact produces significant improvement over the original SDPF-U energies [21].
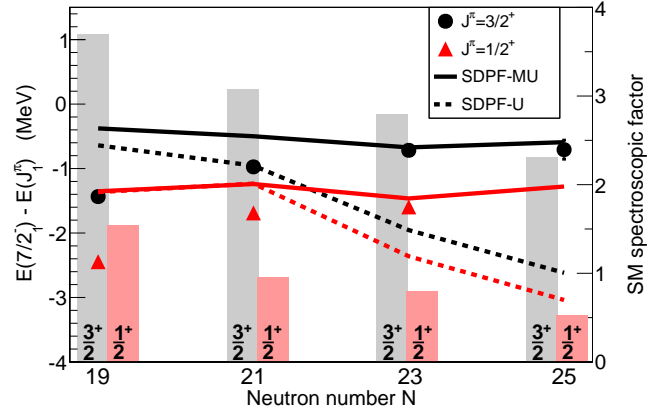

FIG. 5. (color online) Energies of $3/2^+$ and $1/2^+$ intruder states in the silicon isotopes as a function of mass number. The points indicate experimental data, while the lines connect theoretical calculations. The vertical bars show the shell-model spectroscopic factors of the states.

In conclusion, we have exploited one-neutron knockout reactions to probe the evolution of the $f_{7/2}$ and $p_{3/2}$ spectroscopic strength in neutron-rich silicon isotopes. State-of-the-art shell-model interactions describe the trends of the data but underestimate the role of the $p_{3/2}$ orbital. We confirm that the tensor force is necessary to describe the evolution of the $f_{7/2}$ strength, and show that it is
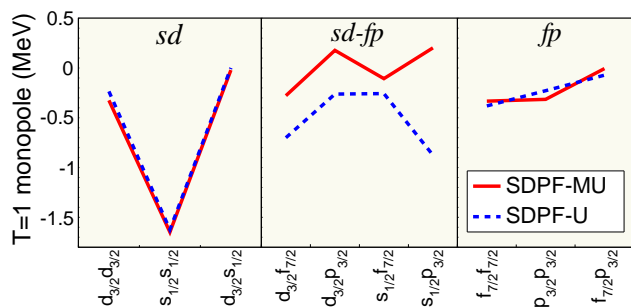
FIG. 6. (color online) Comparison of selected $T = 1$ monopoles terms of the SDPF-U and SDPF-MU effective interactions, evaluated at $A = 42$.

already important at $N = 26$. The observed excess of $p_{3/2}$ strength relative to shell-model predictions indicates that the $N = 28$ shell gap may be reduced even more than present calculations suggest. Neutron cross-shell excitations across the $N = 20$ shell gap were identified and quantified for the first time from the observation of positive-parity final states. The shell-model interactions considered (SDPF-U and SDPF-MU) over-predict the measured $d_{3/2}$ and $s_{1/2}$ neutron removal yields, point-

ing to the deficiency of the applied model space truncations. We have also identified the energies of neutron-hole states which depend strongly on previously unconstrained neutron-neutron monopole interactions. A comparison of shell-model predictions indicates the importance of three-body forces in the evolution of structure in this region.

[1] O. Sorlin and M.-G. Porquet, Prog. Part. Nucl. Phys. **61**, 602 (2008), ISSN 01466410, URL http://linkinghub.elsevier.com/retrieve/pii/S0146641008000380.

[2] T. Otsuka, R. Fujimoto, Y. Utsuno, B. A. Brown, M. Honma, and T. Mizusaki, Phys. Rev. Lett. **87**, 082502 (2001), ISSN 0031-9007, URL http://link.aps.org/doi/10.1103/PhysRevLett.87.082502.

[3] T. Otsuka, T. Suzuki, R. Fujimoto, H. Grawe, and Y. Akaishi, Phys. Rev. Lett. **95**, 232502 (2005), ISSN 0031-9007, URL http://link.aps.org/doi/10.1103/PhysRevLett.95.232502.

[4] A. Zuker, Phys. Rev. Lett. **90**, 042502 (2003), ISSN 0031-9007, URL http://link.aps.org/doi/10.1103/PhysRevLett.90.042502.

[5] T. Otsuka, T. Suzuki, J. D. Holt, A. Schwenk, and Y. Akaishi, Phys. Rev. Lett. **105**, 032501 (2010), ISSN 0031-9007, URL http://link.aps.org/doi/10.1103/PhysRevLett.105.032501.

[6] B. Bastin, S. Grévy, D. Sohler, O. Sorlin, Z. Dombrádi, N. L. Achouri, J. C. Angélique, F. Azaiez, D. Baiborodin, R. Borcea, et al., Phys. Rev. Lett. **99**, 022503 (2007), ISSN 0031-9007, URL http://link.aps.org/doi/10.1103/PhysRevLett.99.022503.

[7] F. Nowacki and A. Poves, Phys. Rev. C **79**, 014310 (2009), ISSN 0556-2813, URL http://link.aps.org/doi/10.1103/PhysRevC.79.014310.

[8] Y. Utsuno, T. Otsuka, B. A. Brown, M. Honma, T. Mizusaki, and N. Shimizu, Phys. Rev. C **86**, 051301 (2012), ISSN 0556-2813, URL http://link.aps.org/doi/10.1103/PhysRevC.86.051301.

[9] E. Caurier, F. Nowacki, and A. Poves, Phys. Rev. C **90**, 014302 (2014), ISSN 0556-2813, URL http://link.aps.org/doi/10.1103/PhysRevC.90.014302.

[10] S. R. Stroberg, A. Gade, J. A. Tostevin, V. M. Bader, T. Baugher, D. Bazin, J. S. Berryman, B. A. Brown, C. M. Campbell, K. W. Kemper, et al., Phys. Rev. C **90**, 034301 (2014), ISSN 0556-2813, URL http://link.aps.org/doi/10.1103/PhysRevC.90.034301.

[11] S. Paschalis, I. Y. Lee, A. O. Macchiavelli, C. M. Campbell, M. Cromaz, S. Gros, J. Pavan, J. Qian, R. M. Clark, H. L. Crawford, et al., Nucl. Instruments Methods Phys. Res. Sect. A Accel. Spectrometers, Detect. Assoc. Equip. **709**, 44 (2013), ISSN 01689002, URL http://www.sciencedirect.com/science/article/pii/S0168900213000508.

[12] C. A. Bertulani and A. Gade, Comput. Phys. Commun. **175**, 372 (2006), ISSN 00104655, URL http://linkinghub.elsevier.com/retrieve/pii/S0010465506001937.

[13] S. Agostinelli, J. Allison, K. Amako, J. Apostolakis, H. Araujo, P. Arce, M. Asai, D. Axen, S. Banerjee, G. Barrand, et al., Nucl. Instruments Methods Phys. Res. Sect. A Accel. Spectrometers, Detect. Assoc. Equip. **506**, 250 (2003), ISSN 01689002, URL http://www.sciencedirect.com/science/article/pii/S0168900203013688http://linkinghub.elsevier.com/retrieve/pii/S0168900203013688.

[14] A. Gade, P. Adrich, D. Bazin, M. D. Bowen, B. A. Brown, C. M. Campbell, J. M. Cook, T. Glasmacher, P. G. Hansen, K. Hosier, et al., Phys. Rev. C **77**, 044306 (2008), ISSN 0556-2813, URL http://link.aps.org/doi/10.1103/PhysRevC.77.044306.

[15] Note1, at ^{40}Si, the effect of the tensor force becomes important relative to the theoretical precision, which is ap-

proximately 10-20% from systematics.

[16] J. Terry, B. A. Brown, C. Campbell, J. Cook, A. Davies, D.-C. Dinca, A. Gade, T. Glasmacher, P. Hansen, B. M. Sherrill, et al., Phys. Rev. C **77**, 014316 (2008), ISSN 0556-2813, URL http://link.aps.org/doi/10.1103/PhysRevC.77.014316.

[17] R. Kanungo, C. Nociforo, A. Prochazka, Y. Utsuno, T. Aumann, D. Boutin, D. Cortina-Gil, B. Davids, M. Diakaki, F. Farinon, et al., Phys. Lett. B **685**, 253 (2010), ISSN 03702693, URL http://www.sciencedirect.com/science/article/pii/S0370269310001693.

[18] K. Wimmer, T. Kröll, R. Krücken, V. Bildstein, R. Gernhäuser, B. Bastin, N. Bree, J. Diriken, P. Van Duppen, M. Huyse, et al., Phys. Rev. Lett. **105**, 252501 (2010), ISSN 0031-9007, URL http://link.aps.org/doi/10.1103/PhysRevLett.105.252501.

[19] Y. Utsuno, T. Otsuka, T. Mizusaki, and M. Honma, Phys. Rev. C **60**, 054315 (1999), ISSN 0556-2813, URL http://link.aps.org/doi/10.1103/PhysRevC.60.054315.

[20] T. Otsuka, T. Suzuki, M. Honma, Y. Utsuno, N. Tsunoda, K. Tsukiyama, and M. Hjorth-Jensen, Phys. Rev. Lett. **104**, 012501 (2010), ISSN 0031-9007, URL http://link.aps.org/doi/10.1103/PhysRevLett.104.012501.

[21] A. Poves, private communication.